SUPPLEMENTAL MATERIAL

Data S1. Supplemental Materials and Methods

Experimental Animals

30-week-old male MFG-E8 KO mice and age-matched WT mice were used in this Ang II infusion study. In addition, 4-, 8-, 20, 50-, and 96-week-old male WT and age-matched KO paraffin archival aortic sections or frozen tissue (in graphs, individual data represents the number of the aortic samples) were employed for the study of age-related arterial remodeling. 10-week-old WT and age-matched KO were utilized for measuring circulating triglyceride, cholesterol, and glucose.

10-week-old male WT, AT1, and AT2 receptor knock out mice (WT, AT1 and AT2 KO, respectively) were provided by Professor Jose Luis Labandeira-Garcia. [43] Mice carrying genetic deletions of the Agtr1 (AT1 KO) gene were obtained from The Jackson Laboratory (Bar Harbor, ME, USA) and Agt2 mice (AT2-KO were generously donated by Dr. Daniel Henrion (University of Angers, Angers, France). [44, 45]

Blood Pressure Measurement

SBP was measured using the pneumatic tail-cuff method (MRBP System, Life Science, Woodland Hills, California). Briefly, animals were placed in a plastic chamber maintained at 34°C and a cuff with a pneumatic pulse sensor was attached to the tail for SBP measurements. Mice were trained for one week to become accustomed to the new handling and environment. Once SBP values were consistent, eight consecutive measurements were performed for each mouse and all the values collected were averaged. Blood pressure was monitored 1 week prior to mini-pump implantation (baseline), and once per week from day 7 to 28 after minipump implantation.

Analysis of Circulating Total Cholesterol, Triglycerides, and Glucose in Untreated WT and KO Mice

Six male 10-weeks-old MFG-E8 KO (KO) and 6 age-matched WT mice were fasted for 16 hours before sacrifice. The mice were anaesthetized via intraperitoneal injection with ketamine (100 mg/kg of body weight) and xylazine (5 mg/kg per body weight). The thoracic cavity was accessed by cutting the sternum to expose the heart, after a 22 G needle attached to a 3 mL syringe was used to puncture the apex of the heart and 800-1,000 µL of blood was collected, representing most of the animal's total blood volume, and was expected to be arterial blood. Blood was collected in heparin tubes (BD, Franklin Lakes NJ, Item# 36664) and placed on ice for 15 minutes. Samples were then spun down at 10,000 rpm for 10 minutes and plasma was harvested and stored at −80°C until use. Total cholesterol, triglycerides and glucose levels were measured from plasma samples according to manufacturer instructions. Assay kits for cholesterol (item# 234-60, lot# 54416), triglycerides (item# 236-660, Lot# 54604) and glucose (item# 235-60, lot# 53909) were obtained from Sekure diagnostics (One Wall Street Burlington, MA 01803 USA), and measured using the Cobas Fara II (Roche Diagnostics Roche Diagnostics Corporation 9115 Hague Rd Indianapolis, IN 46256 USA) chemical analyzer.

Morphometric Analysis of Aortic Walls in Untreated Aging WT and KO Mice

We measured intimal medial thickening (IMT) with aging, by staining archival aortic paraffin sections with hematoxylin and eosin (H&E) from untreated 20-week-old young (WT: n=44; KO: n=40) and 96-week-old aged mice (WT: n=39; KO: n=40). The local renin angiotensin system, including Ang II, AT1 and AT2 receptors, and NF-κB activation, were measured in 8-week-old young (WT: n=4; KO: n=5) and 50-week-old aged mice (WT: n=4; MFG-E8 KO: n=4) using immunohistostaining and Western blotting analyses.

Data S2. Supplemental Results

Ang II, AT1, AT2, and NF-κB Expression in the Arterial wall in Aging Mice

Aortic Ang II protein was significantly increased in untreated aging WT mice, but in the MFG-E8 KO this effect was significantly reduced (**Figure S1A**).

In addition, immunostaining demonstrated that the Ang II receptor AT1 was markedly increased in the aortic walls of untreated WT 96- versus 4-week-old, but the absence of MFG-E8 significantly reduced this age effect; and the Ang II receptor AT2 was markedly decreased in aging WT aortic walls, but the absence of MFG-E8 diminished these effects (**Figure S1B & 1C**). Western blot analysis further confirmed the aging effect on AT1 and AT2 expression (50- versus 8-week-old) (**Figure 1D**).

In addition, Western blotting analysis of aortic protein from 10-week-old male AT1 and AT2 receptor knock out mice indicated that aortic MFG-E8 protein levels were significantly decreased in AT1 KO, but these levels were not altered in AT2 KO mice (**Figure S2**).

NF-κB p65 Expression with Age is Dependent on MFG-E8

Interestingly, immunostaining and Western blotting analysis demonstrated that aging markedly increased the master inflammatory transcription factor p-NF-κB p65 in WT, but MFG-E8 deficiency significantly alleviated this age effect (**Figure S3**).

Ang II Infusion Increases SBP in mice

Increased SBP induced by Ang II infusion was observed in all mice. The repeated, two-way ANOVA analysis showed that SBP had a statistically significant of treatment x genotype interaction ($p<0.0001$) (**Figure S4A).** At baseline (time=day 0) there was no significant difference

in SBP among any of the groups. However, after Ang II infusion, both WT and KO, showed significantly increased SBP levels compared to saline infused mice. Unexpectedly, in KO, the SBP of Ang II infused mice was significantly elevated compared to WT after the infusion ($p<0.01$); and similarly, in KO, the SBP of saline infused was also significantly elevated compared to WT after the infusion ($p<0.01$) **(Figure S4A)**. However, the percentage change of the SBP after Ang II infusion was not significantly altered in KO vs WT (**Figure S4B**), suggesting that Ang II infusion produced a similar hypertensive effect.

Circulating Cholesterol, Triglyceride, and Glucose Profile in Mice

In addition, the baseline blood test results from 10-week-old male WT and KO mice showed that the absence of MFG-E8 significantly decreased plasma cholesterol and triglyceride levels but did not alter plasma glucose levels (**Figure S5**), suggesting that MFG-E8 is involved in lipid metabolism.

Data S3. Supplemental Discussion

Ang II signaling effects on the expression of MFG-E8 during age-associated inflammatory remodeling in mice. The AT1 receptor promotes Ang II inflammatory events while the AT2 receptor blocks Ang II induced inflammation. [43-45] Ang II and AT1 were increased while AT2 was decreased during adverse arterial remodeling in aging mice and was dependent on MFG-E8 (**Figure S1**). Ang II infusion increased the AT1 receptor abundance while it decreased AT2 expression in the arterial wall in mice, which was alleviated by the absence of MFG-E8. In addition, MFG-E8 protein levels were markedly decreased in the AT1 KO mice but are not in the AT2 KO when compared to WT (**Figure S2**). Notably, aging markedly increased the master inflammatory transcription factor p-NF-κB p65 in WT, but MFG-E8 deficiency significantly

alleviated this age effect (**Figure S3**). These findings suggest that the Ang II signaling cascade impacts MFG-E8 expression mainly through the AT1 receptor during age-associated inflammatory remodeling in mice.

Ang II signaling is a key molecular event of age-associated arterial intimal medial thickening. [4, 15,18,19] In the current study, Ang II infusion markedly increased IMT in young WT but not in young KO mice compared to saline infused animals; aging increased IMT in the WT but not in the KO mice; and aging also increased Ang II/AT1 receptor protein expression in the WT but no in the KO animals. These findings indicate that MFG-E8 is required for Ang II-associated vascular intimal medial thickening with aging. Unexpectedly, the KO mice infused with saline had higher levels of IMT than the WT saline control (**Figure 3A**). Notably, at the start of saline infusion, no difference in SBP was observed between the 30-week-old KO and WT animals; however, during the last two weeks of the experiment, SBP levels of the KO animals became elevated when compared to the WT saline (**Figure S4A**). The increased SBP levels during saline infusion could help explain the elevated levels of IMT in the saline infused KO versus WT mice.

MFG-E8 impacts blood pressure in mice. Aortic MFG-E8 is increased in renal hypertensive rats. [46] Increased MFG-E8 is colocalized with increased Ang II protein within old human aortic walls. [4] Ang II infusion increased MFG-E8 in the aortae of mice. These findings suggest that MFG-E8 may influence Ang II associated blood pressure increases. The current study indicated that SBP was increased over a 28-day time course in 30-week-old KO versus WT mice after saline infusion; similarly, SBP was also increased over a 28-day time course in 30-week-old KO versus WT animals after Ang II infusion (**Figure S4A**). However, the percentage change of SBP was not altered in KO versus WT after Ang II infusion (**Figure S4B).** It is well-known that MFG-E8 is a bridging molecule for the clearance of cellular debris by macrophages, and the

absence of MFG-E8 impairs the cleanup of cellular debris, which accumulate and may potentially increase blood pressure in mice. [47] In addition, aging increases MFG-E8 and increases its small, cleaved fragment medin, [7,13,41,42] which is the most common amylogenic protein in aged arterial walls and may potentially induce inflammation and blood pressure increases in old mice.

The inflammatory role of MFG-E8 in the cardiovascular system. There is an apparent contradiction of our current findings which show MFG-E8 promotes an inflammatory role in the arterial wall compared to previous findings which suggests that MFG-E8 exerts an anti-inflammatory role in the heart. [48-50] For example, MFG-E8 attenuates Ang-II induced atrial fibrosis and atrial fibrillation through the inhibition of the TGF-β1/Smad2/3 pathway. [49] MFG-E8 allevaites ventricle fibrosis via the attenuation of endothelial-mesenchymal transition through the Smad2/3/snail signalling pathway. [50] Importantly, restoring circulating MFG-E8 levels retards cardiac hypertrophy through the inhibition of the Akt (protein kinase B, PKB) pathway. [48] In addition, MFG-E8 signaling impacts on adaptive immunity, including the role of anti-inflammation in postischemic cerebral injury. [51] The underlying mechanisms of the inflammatory discrepancies between the heart and arteries is unknown, which need to be further studied.

MFG-E8 is involved in metabolism. MFG-E8 deficiency significantly decreased cholesterol and triglyceride levels (**Figure S5**). The absence of MFG-E8 has been shown to impede the development of obesity by inhibiting the uptake of dietary fat and serum fatty acids in mice. [52] Notably, circulating levels of Ang II post-infusion are significantly higher in KO than WT animals, suggesting that MFG-E8 may be involved in the metabolism of Ang II. The underlying mechanism of MFG-E8-associated metabolism needs to be further investigated.

Supplemental Figures

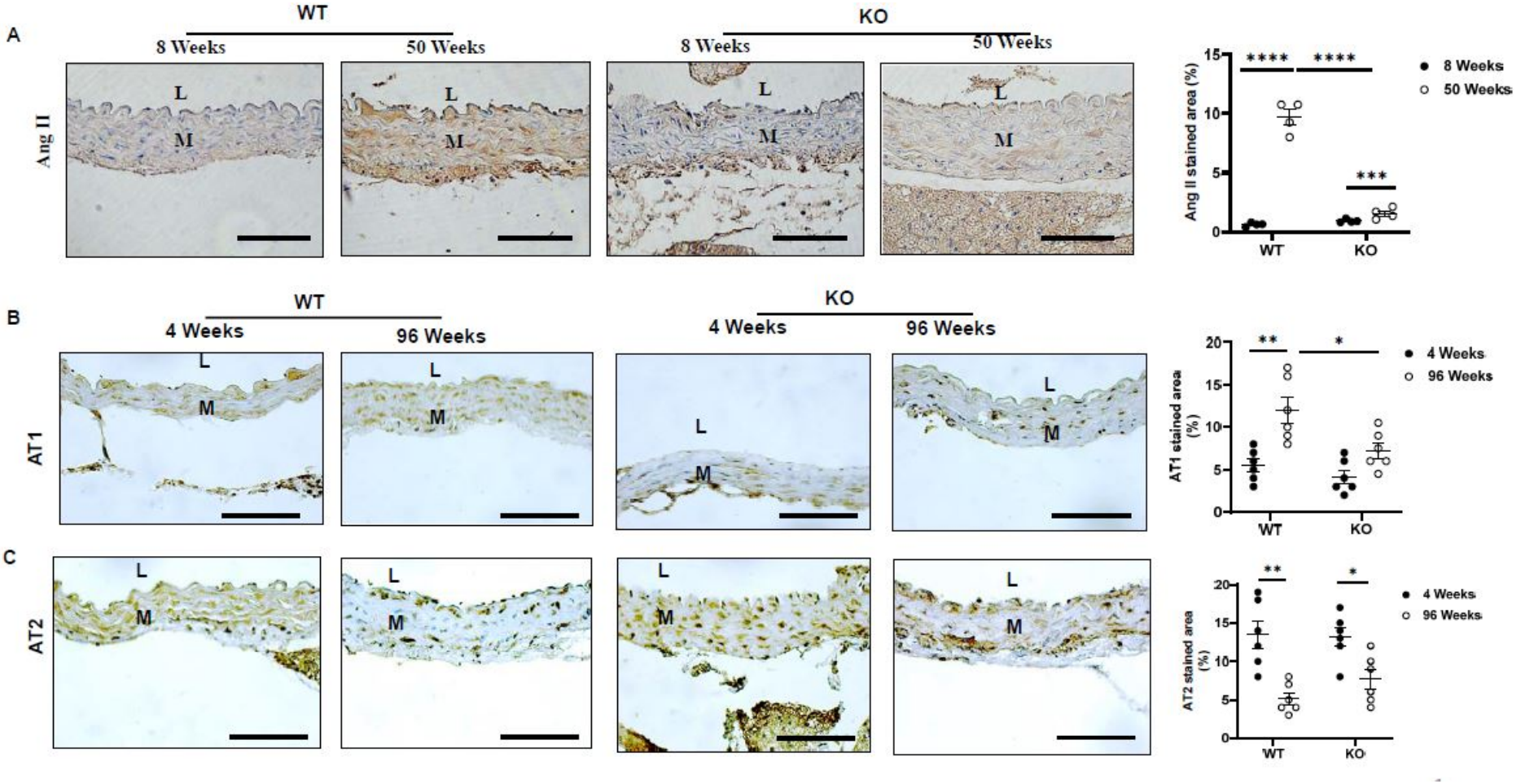

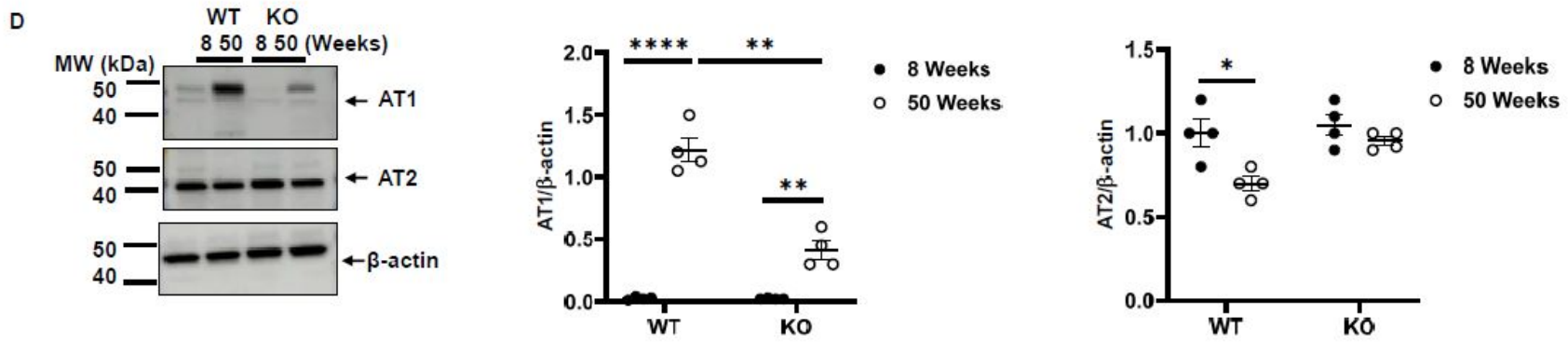

Figure S1. Ang II and AT1/AT2 Expression During Age-Associated Inflammatory Remodeling in Mice. A. Representative photomicrographs of immunostaining of aortic Ang II. Morphometric analysis of Ang II immunostaining in the aortic wall shows Ang II abundance ($p<0.0001$ for main age effect, $p<0.0001$ for main genotype effect, $p<0.0001$ for age x genotype, by two-way ANOVA). Graph showing mean ± SEM combined with individual data points for KO and WT mice. ***=$p<0.001$; and ****=$p<0.0001$ by Bonferroni post-hoc tests following two-way ANOVA. L=lumen; M=media. Scale bar = 100μm. **B.** Representative photomicrographs of immunostaining of the Ang II AT1 receptor. Morphometric analysis of the AT1 immunostaining in the aortic wall ($p<0.01$ for main age effect, $p<0.001$ for main genotype effect, by two-way ANOVA). Graph showing mean ± SEM combined with individual data points for KO and WT mice. *=$p<0.05$ and **=$p<0.01$ by Bonferroni post-hoc tests following two-way ANOVA. **C.** Representative photomicrographs of immunostaining of the aortic Ang II AT2 receptor. Morphometric analysis of AT2 abundance ($p<0.0001$ for main age effect, by two-way ANOVA). Graph showing mean ± SEM combined with individual data points for KO and WT mice. *=$p<0.05$ and **=$p<0.01$ by Bonferroni post-hoc tests following two-way ANOVA. **D.** Representative Western blots of the AT1 and AT2

receptors (left panels). Western blotting analysis of the AT1 abundance ($p<0.0001$ for main age effect, $p<0.0001$ for main genotype effect, $p<0.0001$ for age x genotype, by two-way ANOVA). Graph (middle panel) showing mean ± SEM combined with individual data points for KO and WT mice. **=$p<0.01$and ****=$p<0.0001$ by Bonferroni post-hoc tests two-way ANOVA. Western blotting analysis of the AT2 abundance (right panel) ($p<0.05$ for main age effect, $p<0.01$ for main genotype effect, by two-way ANOVA). Graph showing mean ± SEM combined with individual data points for KO and WT mice. *=$p<0.05$ by Bonferroni post-hoc tests following two-way ANOVA. L=lumen; M=media. Scale bar = 100 μm.

Figure S2. Effects of Ang II receptors on MFG-E8 expression in the aortic wall of mice. Representative Western blots (left panel) of aortic MFG-E8 from 10-week-old AT1 and AT2 KO mice. Western blotting analysis of MFG-E8 abundance ($p<0.001$ for the genotype effect, by one-way ANOVA). Graph (right panel) showing mean ± SEM combined with individual data points for KO and WT mice. ****=$p<0.0001$ by Bonferroni post-hoc tests following one-way ANOVA.

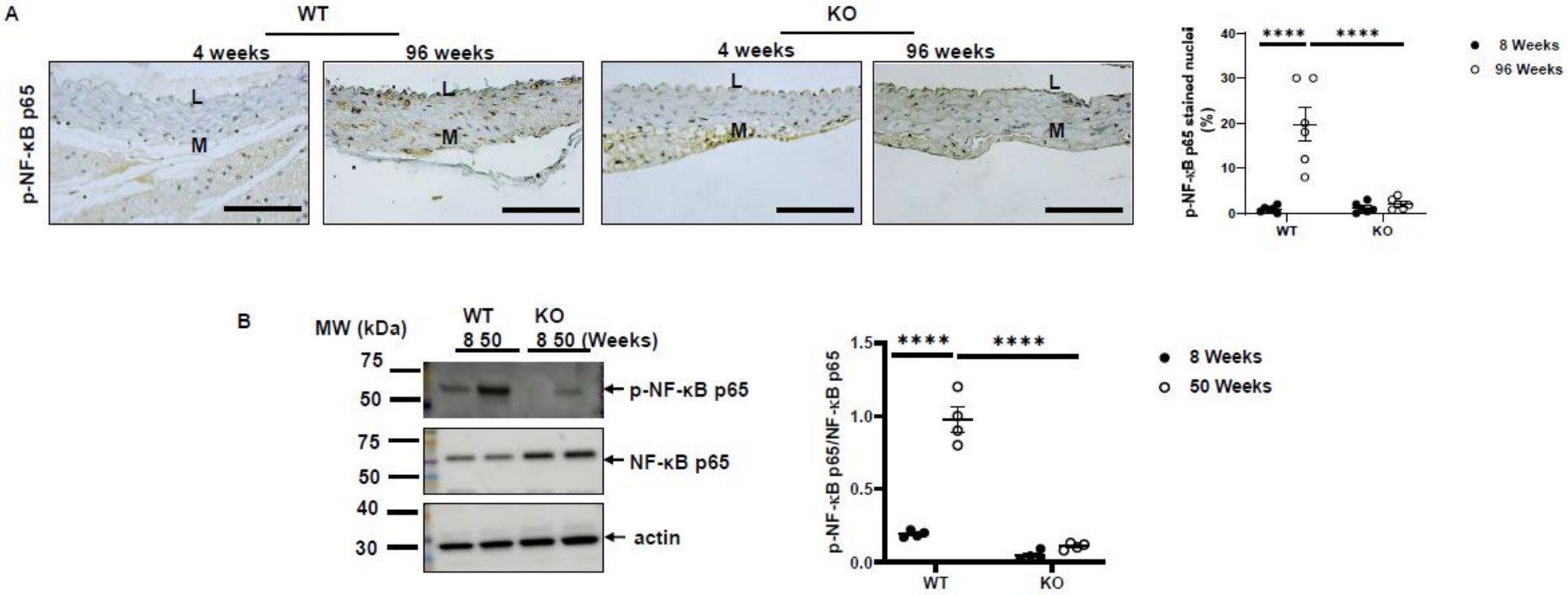

Figure S3. The age-associated activation of NF-κB in the aortic wall of mice. A. Representative photomicrographs of immunostaining of aortic p-NF-κB p65. Morphometric analysis of the percentage of p-NF-κB p65 stained nuclei in the aortic wall ($p<0.001$ for main age effect, $p<0.0001$ for main genotype effect, $p<0.001$ for age x genotype, by two-way ANOVA). Graph showing mean ± SEM combined with individual data points for KO and WT mice. ****=$p<0.0001$ by Bonferroni post-hoc tests following two-way ANOVA. **B.** Representative Western blots of NF-κB p65 (left panel). Western blotting analysis of the p-NF-κB p65 abundance

($p<0.0001$ for main age effect, $p<0.0001$ for main genotype effect, $p<0.0001$ for age x genotype, by two-way ANOVA). Graph (right panel) showing mean ± SEM combined with individual data points for KO and WT mice. *=$p<0.05$ and ****=$p<0.0001$ by Bonferroni post-hoc tests following two-way ANOVA. L=lumen; M=media. Scale bar = 100 μm.

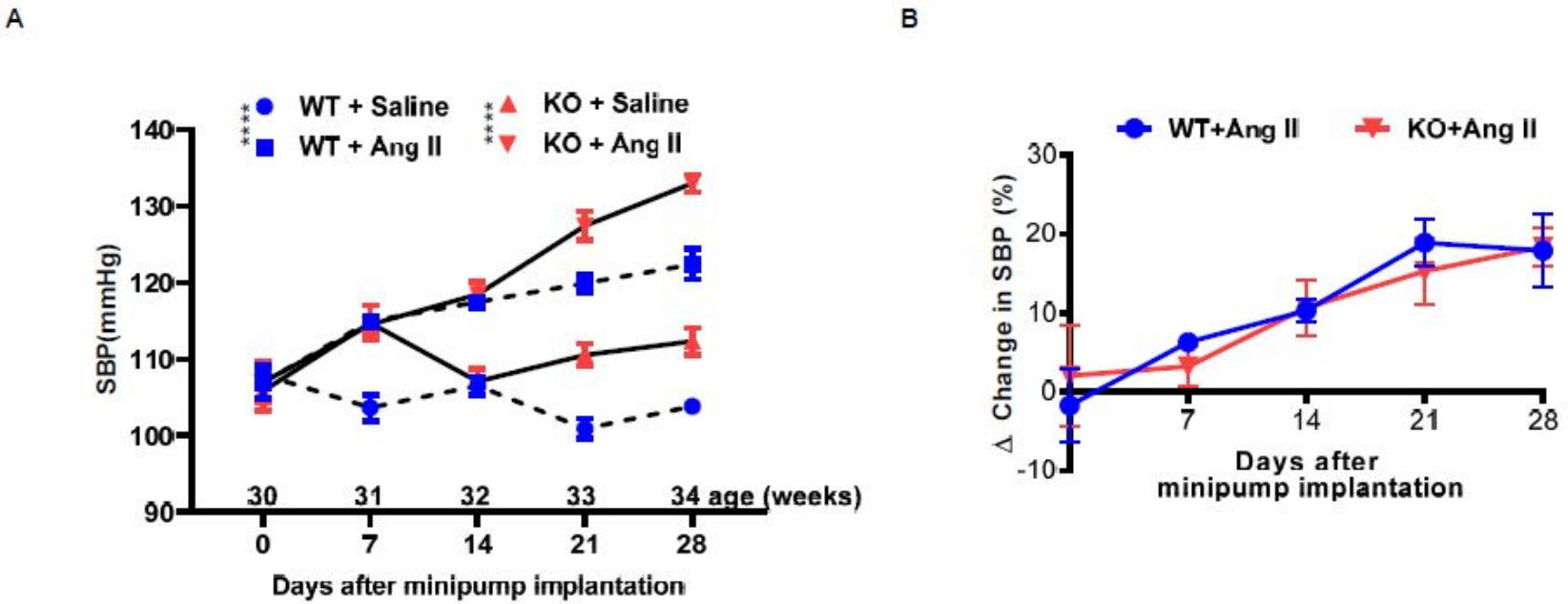

Figure S4. Dynamic changes in systolic blood pressure in mice. A. Dynamic changes in mouse SBP measured by tail-cuff method; plot shows mean ± SEM for KO and WT mice (n=5/group) with Ang II or saline infusion over time ($p<0.001$ for main treatment effect, $p<0.001$ for main genotype effect, $p<0.001$ for Ang II infusion x genotype, by repeated two-way ANOVA and a linear mixed-effects model). ****=$p<0.0001$ SBP in KO + Ang II vs KO + saline and WT + Ang II vs WT + saline group. **B**. Dynamic percentage changes in mouse SBP as measured by tail-cuff method; graph showing mean ± SEM for KO and WT mice (n=5/group) with Ang II or saline infusion over time, $p>0.05$, analyzed by repeated two-way ANOVA.

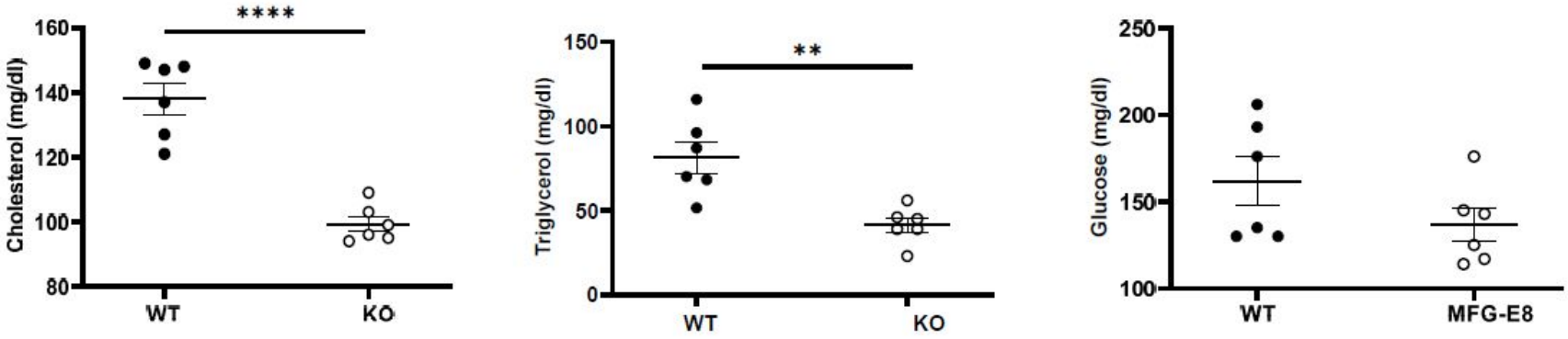

Figure S5. Circulating cholesterol, triglyceride, and glucose in mice. Plasma cholesterol (left panel), triglyceride (middle panel), and glucose (right panel). Graph showing mean ± SEM combined with individual data points for KO and WT mice. ** =$p<0.01$ and ****=$p<0.0001$ by unpaired t-test.